

---

---

STATISTICAL  
RADIOPHYSICS

---

---

## Radar Reflections from a Clear Sky in the 35 GHz Range

V. V. Sterlyadkin<sup>a, \*</sup>, K. V. Kulikovskii<sup>a</sup>, V. M. Kalmykov<sup>b</sup>, and D. V. Ermilov<sup>b</sup>

<sup>a</sup> Russian Technological University MIREA, Moscow, 119454 Russia

<sup>b</sup> Central Design Bureau of Apparatus Engineering, Tula, 300034 Russia

\*e-mail: sterlyadkin@mail.ru

Received September 16, 2020; revised September 16, 2020; accepted February 24, 2021

**Abstract**—The operating experience of a wind profiler operating at a frequency of 35 GHz is considered. Particular attention is paid to radar reflections from the clear sky (angels), which can be detected down to a level of  $-60$  dBZ. We showed that, in some cases, clear-sky signals cannot be interpreted within the framework of the traditional theory of reflections from turbulent irregularities. The impossibility of interpreting the received signals as reflections from insects or large aerosols is statistically substantiated. Various putative sources of clear-sky reflections in a given wavelength range are considered.

DOI: 10.1134/S1064226921090163

### INTRODUCTION

Radar reflections from a clear, cloudless atmosphere (sometimes called “angels”) are the least studied phenomena in radar meteorology and statistical radiophysics. This is especially true for the millimeter wavelength range, which began to be widely used for meteorological purposes only in the last 10–15 years. The first meteorological radar measurements carried out in the 1950–1960s of the 20th century showed that radio echo is formed not only from precipitation or clouds, but often from a visually transparent clean atmosphere [1–3]. During the research, it was revealed that the sources of such reflections can be visually unobservable scatterers: birds, insects, plant seeds carried away by air flows, large aerosols, as well as inhomogeneities in the refractive index of air [3, 4]. The latter can be conditionally divided into layered horizontally extended formations at the boundaries of which the gradients of the refractive index are formed [5, 6]. Another type of reflection is associated with turbulent inhomogeneities that are distributed over the space volume [6, 7]. Layered irregularities usually form a reflected signal the power of which is maximum at specular reflection and decreases very quickly when deviating from this condition. Usually, radar reflections in the meter and decimeter wavelength ranges have this character. For this reason, meter and decimeter profilers (in the English language literature they are called profiler) usually carry out sounding at elevation angles close to the zenith, with a beam deviation from vertical by  $10^{\circ}$ – $20^{\circ}$ . Reflections distributed over the volume are associated with Bragg scattering by turbulent vortices with a scale equal to half the wavelength [6–8]. There is a minimum vortex size below which the vortices are destroyed by viscous fric-

tion. For the lower troposphere, this scale, according to estimates by various authors, is a few millimeters and increases with height, reaching decimeter scales in the upper troposphere. When operating in the 35 GHz frequency range (wavelength 8.6 mm), we find that the size of turbulent vortices should not exceed 4 mm, and this value is at the lower limit of applicability of the turbulent scattering theory for the troposphere. Under such boundary conditions, the use of classical formulas can lead to errors, since other scattering mechanisms can also be included into play. To study this very topical problem, special comprehensive studies, the accumulation of statistical material and its careful analysis are required. This paper presents the experimental results of measurements of radar reflections from a clear atmosphere, obtained using a Doppler radar station (radar) in the 35 GHz range. The analysis of the level of radar reflectivity and statistical properties of signals was carried out, however, complex studies were not carried out. It should be noted that the use of the millimeter wavelength range for meteorological purposes has been widely used only in the last 10–15 years [9, 10]. In Russia, research on the use of millimeter waves to create a wind radar began earlier than abroad. In the early 2000s, the research “Mechanism” was carried out in Moscow State University of Instrument Engineering and Computer Science (now Russian Technological University, MIREA). In 2004, at the Central Design Bureau of Apparatus Engineering (CDBAE) in Tula, the first 35 GHz model of a small-sized wind-sounding radar complex was created [11, 12]. Already the first field measurements showed that the range of meteorological conditions under which its application is possible turned out to be much wider than predicted by theoretical estimates and the

experience of using longer-wave radars. Radar signals were formed in the 300–500 m layer in almost 80% of cases, including in clear weather. In addition, the potential of the radar made it possible to receive signals from almost all types of clouds, which, along with surface data, made it possible to reconstruct the wind profile from below to the upper cloud limit. Considering that in central Russia, cloudiness is observed in more than 70% of cases, it turned out that the created radar is an effective means of wind sounding of the troposphere.

## 1. MEASUREMENT INSTRUMENTATION AND TECHNIQUE

A detailed description of the technical characteristics of the radar, which has the working name of the probeless wind profiler (PWP), is given in [12–14]. Here, we will briefly describe only the part that concerns the assessment of the meteorological potential of the radar and the methodology for measuring the radar reflectivity of meteorological objects.

The sounding mode consists of conducting an azimuthal section at constant elevation angle  $\beta = 45^\circ$ , with 12 discrete values of azimuth angle  $\alpha_i = 0^\circ, 30^\circ, \dots, 270^\circ$ . The pulse power radiated into space was  $P_{\text{pulse}} = 3.5$  kW, the duration of the probing pulses was  $\tau = 0.4$   $\mu\text{s}$  (the resolution in the range was 60 m and in the height was 42.6 m), the repetition frequency could be switched to  $f_{\text{rep1}} = 12.5$  kHz or  $f_{\text{rep2}} = 25$  kHz. In each of the 12 sounding directions, the signal was accumulated for 6 s, which made it possible to analyze either 75000 or 150000 pulses at each discrete height  $H_j$ , where  $j = 1-200$  or  $j = 1-100$ . Considering that the width of the distribution over the projections of velocities  $\Delta v$  in the probed volume almost always exceeds 0.4–0.5 m/s, the width of the Doppler spectra will be equal to

$$\Delta f_D = \frac{2\Delta v}{\lambda} \geq 100 \text{ Hz.}$$

Consequently, the optimal duration of one realization under the fast Fourier transform should be

$$\Delta \tau_{\text{opt}} = \frac{1}{\Delta f_D} = 0.01 \text{ s.}$$

Taking into account two possible pulse repetition rates, this corresponds to dividing the signal into realizations according to  $M_1 = 128$  or 256 samples. The accumulation of signals for 1 s in each direction of sounding will provide further incoherent accumulation of  $M_2 = 6 \text{ s}/0.01 \text{ s} = 600$  spectra for each selected element of the space volume.

In accordance with [7], the radar equation for meteorological radars with a parabolic antenna can be represented as follows:

$$P_r = \frac{0.28\lambda^2 P_t G^2 h \theta^2 k_1 k_2 \eta k k_3}{(4\pi)^3 R^2} = \frac{P \eta k k_3}{R^2}. \quad (1)$$

Here,  $P_r$  is the power of the received signal;  $P_t$  is the power of the emitted pulse;  $G$  is the gain of the transmitting/receiving antenna;  $h = c\tau_{\text{pulse}}$  is the length of the irradiated volume;  $\theta$  is the width of the antenna directional pattern;  $\eta$  is the specific radar reflectivity per unit volume;  $k_1$  and  $k_2$  are coefficients that take into account losses in the radar paths and its non-optimal reception mode, respectively;  $k$  is a coefficient that takes into account the attenuation of the signal when passing twice the atmosphere;  $k_3$  is a coefficient that takes into account the degree of filling of the scattering volume; and  $R$  is the range of the scattering volume. All parameters characterizing the radar are usually combined into constant  $P$ , which is called the meteorological potential of the radar. Taking into account the effective area of antenna aperture  $A_r = 0.95 \text{ m}^2$ , we obtain the antenna gain equal to

$$G = \frac{4\pi A_r}{\lambda^2} = 1.6 \times 10^4.$$

For the created version of the PWP radar, it is necessary to take into account the level of losses in paths  $k_1 = 0.5$  and the possible suboptimality of signal processing mode  $k_2 = 0.4$ . As a result, we find that the meteorological potential of the created radar is  $P = 1.4 \times 10^3 \text{ m}^3 \text{ W}$ .

To determine the detection capabilities of the created radar, it is necessary to calculate the level of minimum detectable signal  $P_{\text{min}}$ , which depends on the characteristics of the receiver and the signal accumulation time. The noise power at the output of the receiving system can be estimated by relation:  $P_n = k T_0 F_n B_n$ . The noise factor of the receiving system is equal to  $F_n = 4.0$ ,  $T_0 = 290$  K, and the optimal bandwidth of the receiver is  $B_n = 1/\tau_{\text{pulse}} = 2.5 \times 10^6$  1/s. The optimal processing mode means coherent accumulation of the signal within the signal coherence time, i.e. during  $\Delta \tau_{\text{coh}} = 1/\Delta f_D = 0.01$  s. This corresponds to the duration of one implementation. With a repetition rate of 25 kHz, one implementation will have  $M_1 = 256$  pulses, then, taking into account the quadrature analysis, we will get the same number of points of the Doppler spectrum. In this case, all the noise power is distributed on  $M_1$  points of the spectrum, which leads to a decrease in the noise power per element of the Doppler spectrum resolution by a factor of  $M_1$  (from this moment we turn to the terminology of spectral density, the power referred to the Doppler resolution step). Note that the entire signal power is recorded in

one element of the Doppler spectrum. The incoherent accumulation of Doppler spectra for 6 s allowed the incoherent accumulation of  $M_2 = 6 \text{ s}/0.01 \text{ s} = 600$  spectra, which gives a gain in the signal-to-noise ratio (SNR) by factor of  $\sqrt{M_2}$ . The experience of processing Doppler spectra shows that for signal recognition it is sufficient that the SNR in the spectrum is  $\text{SNR} = 3$ . As a result, it is easy to calculate the power of the minimum detectable signal falling on the minimum frequency interval of the Doppler spectrum:

$$P_{\min} = P_n (S/N) \frac{1}{M_1 \sqrt{M_2}} = 1.95 \times 10^{-17} \text{ W}. \quad (2)$$

If we use the definition of potential (1), then it is easy to calculate the minimum value of the specific radar reflectivity that a wind radar can register at altitude  $h = 1000 \text{ m}$  (distance  $R = 1410 \text{ m}$ ).

$$\eta_{\min} = \frac{P_{\min} R^2}{P} = 2.8 \times 10^{-14} \text{ m}^{-1}. \quad (3)$$

This value can be converted to equivalent radar reflectance  $Z$ , assuming that the signal is formed by a drop of water [7]:

$$\eta = \frac{\pi^5}{\lambda^4} |K_w|^2 \beta Z, \quad (4)$$

where  $|K_w|^2 = 0.8 - 0.95$  for water droplets,  $\beta = 10^{-18}$  takes into account the transition of dimensions in the value of  $Z$  to  $\text{mm}^6/\text{m}^3$ . For our system, taking into account, we obtain

$$\eta (\text{m}^{-1}) = 5.6 \times 10^{-8} Z \left( \frac{\text{mm}^6}{\text{m}^3} \right). \quad (5)$$

Thus, on the basis of the presented data, it turned out that the theoretical value of the meteorological potential of the radar is such that it allows recording a signal from objects with specific radar reflectivity  $\eta = 2.8 \times 10^{-14} \text{ m}^{-1}$  or  $Z_{\min} (h = 1 \text{ km}) = -63 \text{ dBZ}$  at an altitude 1 km.

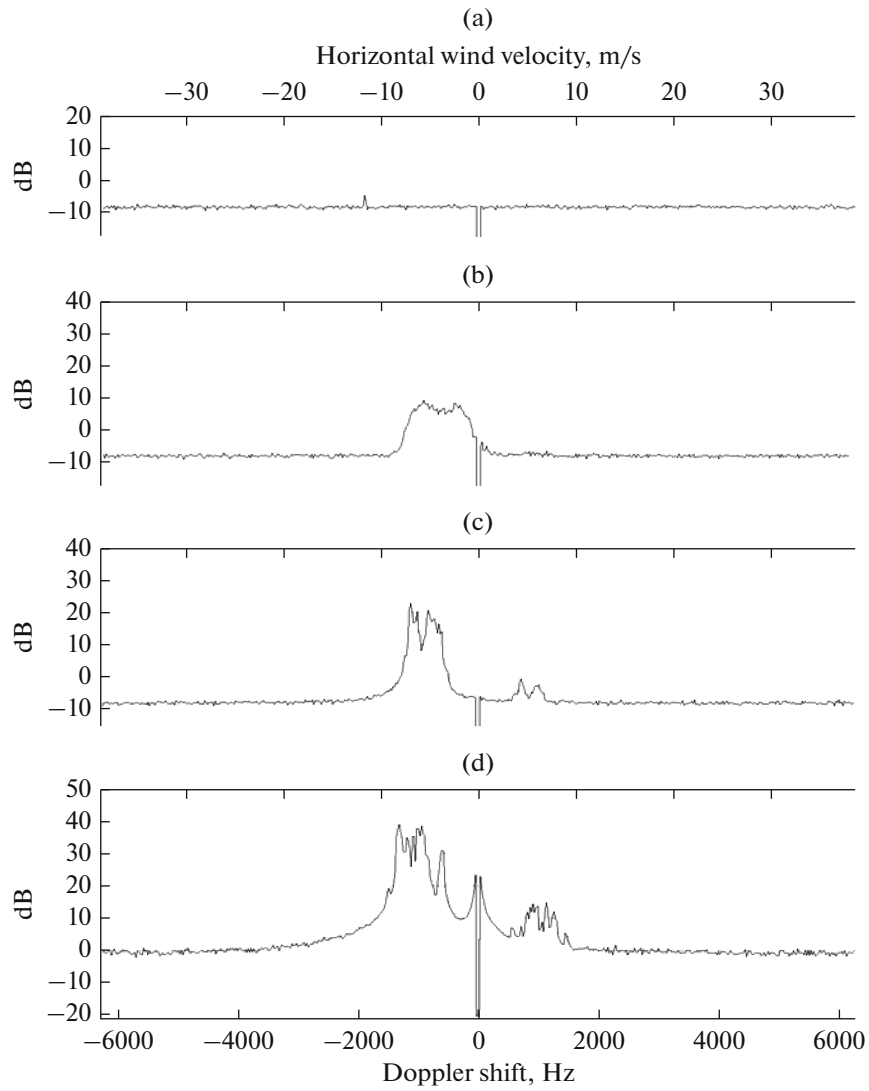
The theoretical assessment of the meteorological potential of the wind radar was confirmed by complex radar-radiometric measurements of clouds [15]. The physical basis of such measurements was the fact that the water content of the cloud can be estimated from the radiometric contrast that occurs between the cloudless zone of the sky and the zone with a cloud of good weather "Cumulus Humilis." In this case, the radar reflectivity obtained by a radar operating at the same wavelength, in turn, is associated with the water content of the cloud [7]. As a result, it is possible to estimate the potential of the radar by joint measurements of the reflectivity contrasts and the radiometric contrast created by the cloud [15]. The results of complex measurements made it possible to estimate the minimum value of the effective radar reflectivity that the radar can record at an altitude 1 km with value

$Z_{\min} (h = 1 \text{ km}) = (-58 \pm 5) \text{ dBZ}$ . Compared to the theoretical estimate based on the radar parameters, the resulting value differs by 4 dB. We will take the average value between the theoretical calculation and the experimental estimate as true value  $Z_{\min} (h = 1 \text{ km}) = (-60 \pm 5) \text{ dBZ}$ .

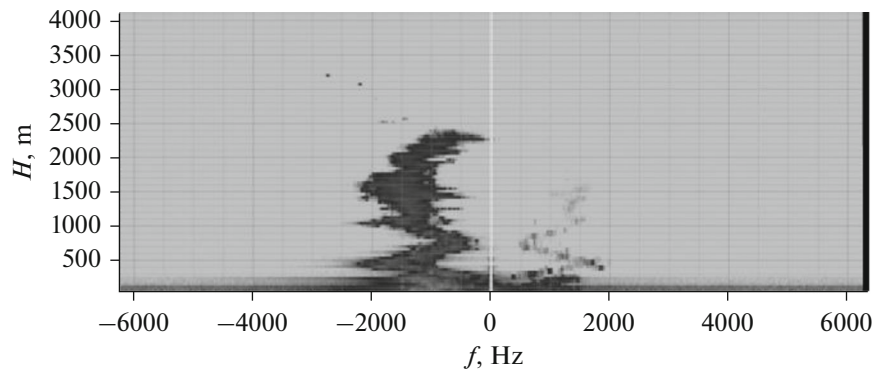
Next, we will consider the technique for measuring the vertical profile of the effective radar reflectivity. Figure 1 shows examples of Doppler spectra measured in clear-sky conditions near the Baikonur cosmodrome on July 1, 2017 at 16:05 Moscow time. Spectral density is presented in relative units on a logarithmic scale.

Figure 2 shows a spectrogram obtained for the selected direction of sounding, which combines all Doppler spectra into one demonstrative plot. In this case, each line of the spectrogram represents a spectrum at the corresponding height, and the spectral power density is depicted by the shading density. It should be noted that in this example, the width of the spectra obtained under clear-sky conditions up to an altitude 2200 m sometimes reaches 3–4 m/s, which is more than is usual in the case of clouds or precipitation.

On the spectra, presented on a logarithmic scale, at high signal levels, a symmetrical part of the spectrum is visible, which is 25 dB below the true signal. This is due to incomplete suppression of the signal during quadrature processing. It should be noted that the level of the noise track depends on the range and, to a lesser extent, on the direction of sounding. At the lowest altitudes, this level increases by 6–8 dB compared to altitudes greater than 250 m. Apparently, this is due to reflections from local objects falling into the side lobes of the antenna. For this reason, we also measured the level of the useful signal from the average noise level in the spectral regions that are far from the region of possible signals. Approximately the same methodology for assessing the noise level was used in [16]. At the same time, rms spectral noise density  $\sigma_n$  was calculated in the same areas. The power of the radar signal is calculated in relative units as an integral of the Doppler spectrum, which exceeds the average noise level plus  $3\sigma_n$ . Noise during such processing was not included in the calculation of the signal level. However, increasing the noise level does not change the signal strength, so simply subtracting the noise track and integrating the remaining spectrum will underestimate the signal. In this regard, in the calculations, the signal power was corrected for the difference arising from the rise in the noise level. To convert the signal power into radar reflectivity, it was multiplied by the square of the height. The resulting radar reflectivity, expressed in relative units, was normalized to the radar potential so that at a distance of 1 km the minimum signal level was  $-60 \text{ dBZ}$ .



**Fig. 1.** Typical shape of Doppler spectra obtained under clear-sky conditions at the Baikonur cosmodrome (on July 1, 2017 at 16:05 Moscow time) at heights of 3742 (a), 2257 (b), 857 (c), and 51 m (d).



**Fig. 2.** Spectrogram, each line of which is a Doppler spectrum at a given height.

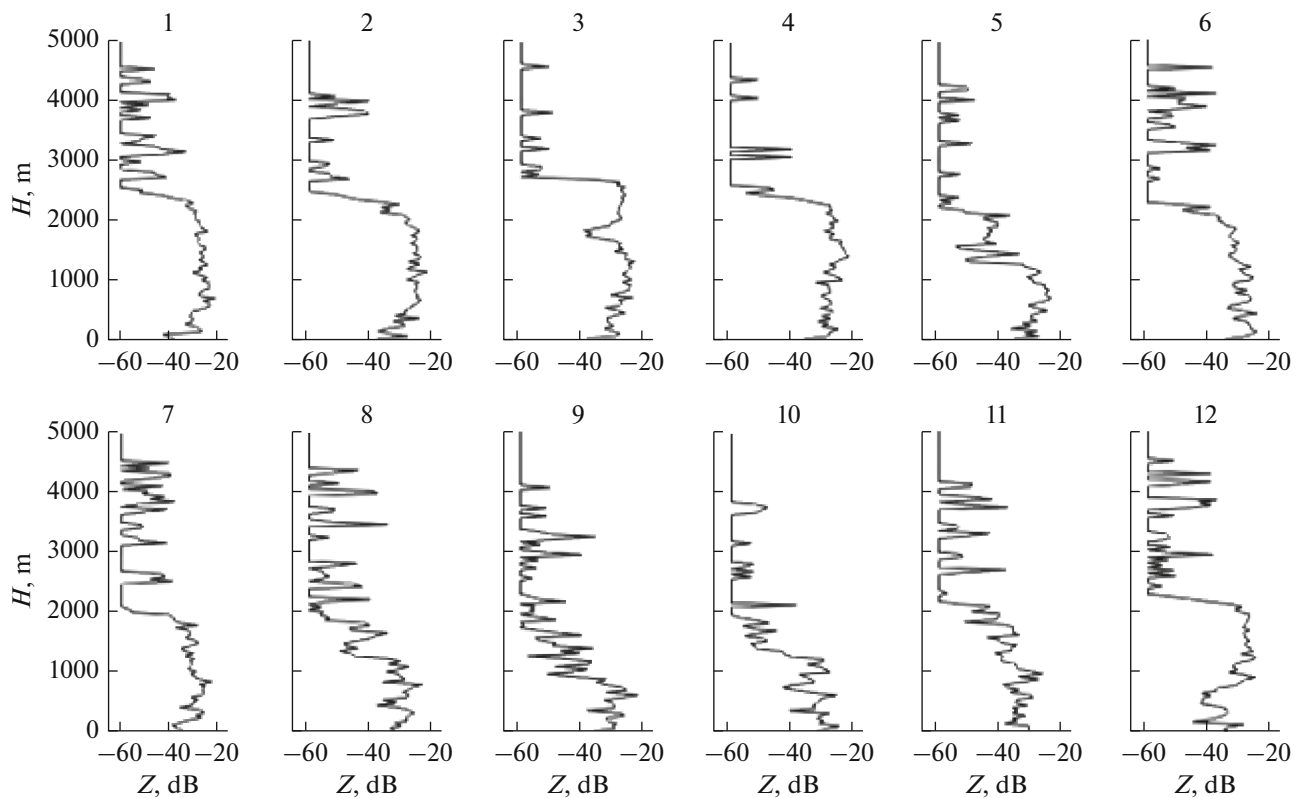


**Fig. 3.** Dependences of clear sky radar reflectivity on altitude for 12 different azimuthal sounding directions obtained at the Baikonur cosmodrome on July 1, 2017 at 16:04 Moscow time.

## 2. MEASUREMENT RESULTS OF RADAR REFLECTANCE FOR VARIOUS CLEAR SKY EXAMPLES

Consider examples of measurements taken under clear sky conditions in the summer months of the year. In Fig. 3, on a logarithmic scale, the dependences of radar reflectivity on altitude for ten different directions obtained near the Baikonur cosmodrome on July 1, 2017 at 16:04 Moscow time are presented. The surface temperature was 26°C. Similar measurements were obtained in the vicinity of Tula on June 16, 2016 at 12:51 Moscow time (Fig. 4). The temperature on the ground was 28°C. The plots show a general underestimation of the reflectivity in the 50–250 m layer, which is apparently associated with an increase in the level of the noise track in this height interval. The common property for both measurements are: firstly, a high average level of radar reflectivity  $Z = -30$  to  $-20$  dBZ up to an altitude of 2000–2200 m, and secondly, uniformity of radar reflectivity in this altitude range. So, in Fig. 3 in 7 directions out of 12, and in Fig. 4 in all 12 directions in the altitude range of 500–2000 m, the radar reflectivity is kept in a very narrow interval ( $-35 \pm 5$ ) dBZ.

It should be noted that the very high value of radar reflectivity, which is stable in space and time, is close to the reflectivity of clouds.

### 2.1. Interpretation of Results and Analysis of Possible Sources of Clear-Sky Reflections

Reflections from a clear cloudless sky are traditionally divided according to the types of reflection sources. It has been shown that reflections can be formed by birds, insects, plant seeds carried away by air currents, aerosols, and fluctuations in the refractive index of air [1–7]. Reflections from seeds and large aerosols, on average, obey the Boltzmann distribution over height and, even in the presence of vertical flows, should decrease exponentially with height. This does not happen in our examples. Therefore, this reason for the formation of signals should be discarded.

The peculiarity of reflections from birds and insects point reflections and do not fill the entire sensing area but are noted at certain distances and in certain directions. In our examples, the reflections are volumetric and uniformly fill the entire layer up to a height of 2000 m. Therefore, a natural assumption is to interpret the signals as reflections from fluctuations in the refractive index. The theory of such reflections in the microwave wavelength range was developed by V.I. Tatarskii in his fundamental study [17]. It shows that turbulent fluctuations of the refractive index (within the inertial range of turbulence) form in space many periodic structures of various scales. Microwaves undergo Bragg-type backscattering from peri-

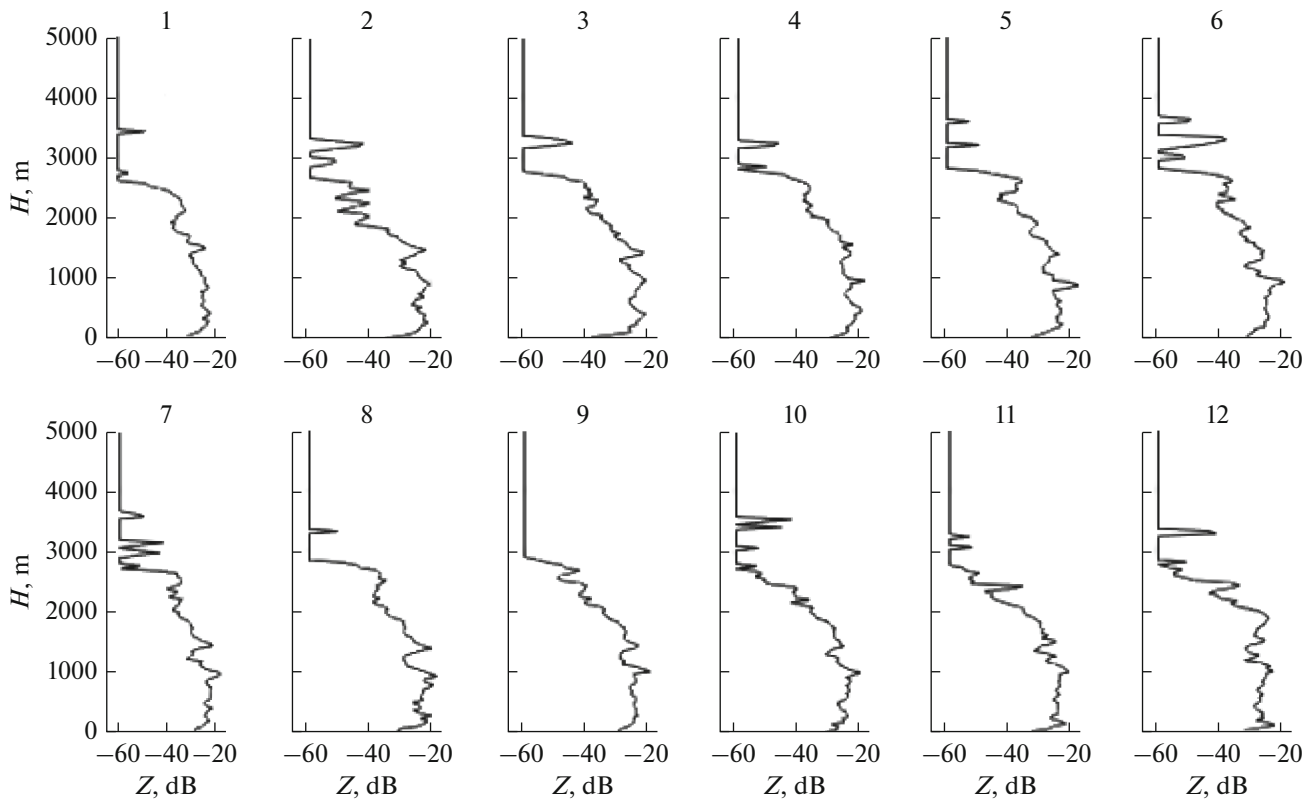


Fig. 4. Dependences of clear sky radar reflectivity on altitude for 12 different azimuth sounding directions, obtained on June 16, 2016 at 12:51 Moscow time (Tula).

odic inhomogeneities in the refractive index, the size of which is half the wavelength. A relation is obtained for calculating the specific scattering area (specific reflectivity) of developed turbulence [7, 17]:

$$\eta = 0.38C_n^2\lambda^{-1/3}, \tag{6}$$

where  $\eta$  is expressed in  $m^{-1}$ ,  $C_n^2$  is a measure of the intensity of fluctuations of the refractive index and has the dimension of  $m^{-2/3}$ , and  $\lambda$  is the wavelength, in m.

In [17], a large number of experimental data are presented, which confirm the developed theory as applied to wavelengths of 3 cm and above. Collected experimental material [17, p. 434] showed that  $C_n^2$  can vary in the range from  $C_n^2 = 2 \times 10^{-14} - 10^{-16} \text{ cm}^{-2/3}$  to  $4.3 \times 10^{-13} - 2.1 \times 10^{-15} \text{ m}^{-2/3}$ . The data obtained during the year on the 10 cm radar [18] show the maximum values of  $C_n^2$  an order of magnitude less. We take maximum value  $C_n^2 = 4.3 \times 10^{-13} \text{ m}^{-2/3}$  and, by relation (6), we obtain the maximum theoretical value of the specific reflectance for a wavelength  $\lambda = 8.6 \text{ mm}$ :

$$\eta_{\max} = 8.0 \times 10^{-13} \text{ m}^{-1}. \tag{7}$$

If, according to formula (5), this value is converted into effective radar reflectivity  $Z$ , then we obtain

$$Z_{\max} = 1.4 \times 10^{-5} \frac{\text{mm}^6}{\text{m}^3} = -49 \text{ dBZ}.$$

Obviously, in the cases under consideration, with a weak wind ( $V < 10 \text{ m/s}$ ), the intensity of turbulence should not take extreme high values and the radar reflectivity formed by turbulent pulsations should be several times less, at the level from  $-55$  to  $-65 \text{ dBZ}$ . These values are at the edge of the radar sensitivity and should hardly be recorded by it. Nevertheless, in the cases under consideration, in a layer up to 2 km, we register  $Z$  at a level of  $-35 \pm 5 \text{ dBZ}$ . These values are 15–20 dB higher than theoretical estimates! This discrepancy can hardly be attributed to the error in assessing the potential of the radar, since our radar registers all types of clouds up to 12 km, which is impossible for low-potential radar. A similar potential is demonstrated by foreign millimeter-wave radars [19, 20].

Let us consider in more detail the version that, in principle, can explain the noted discrepancy. These are reflections from small insects, the scattering cross section of which is well within the observed values. However, the statistical properties of the observed sig-

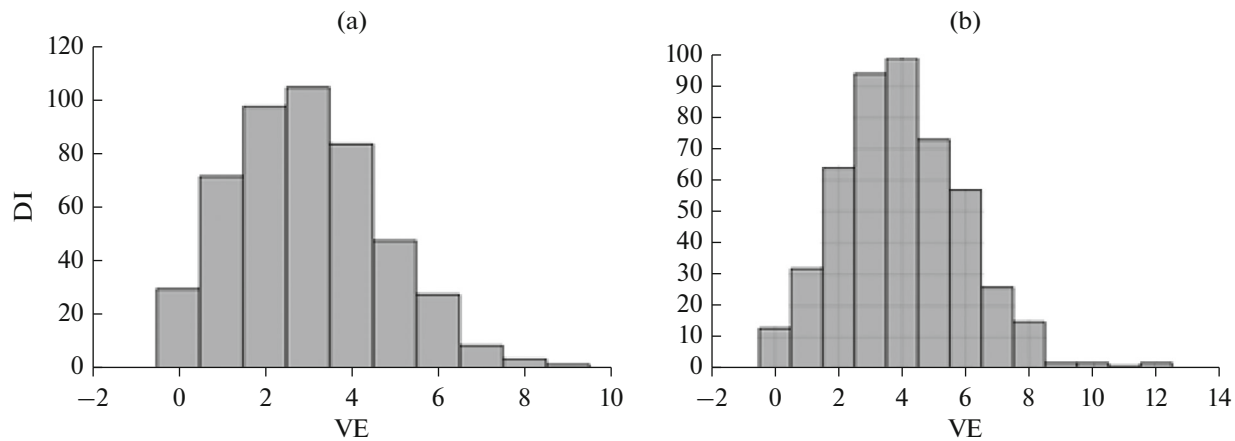


**Fig. 5.** Distribution of insects (DI) by volume elements (VE) at  $N = 1440$  (a) and  $N = 1920$  individuals (b) in 480 volume elements. In each case, there are insect-free volume elements.

nals are such that the insect version is not consistent [21]. From Figs. 3 and 4 it follows that the distribution of reflectivity is almost uniform in all elements of the radar resolution up to an altitude of 1600–2000 m. In this case, such statistical properties of the signal cannot be explained only by the appearance of insects in the sounding volume. The fact is that the distribution of insects in space cannot be uniform, provided that only a few individuals fall into the probe volume. Necessarily, due to the random distribution and flocking behavior of insects, in some volumes there will be a large number of insects, and in some they will not be at all. Accordingly, the intensity of the radar signal will fluctuate strongly from background values, determined by reflections from fluctuations of the refractive index, to very significant ones, determined by the presence of insects. In our measurements, in the entire area from 50 to 1600 m (with a step of 40 m) and in all 12 sounding directions, the radar reflectivity did not fall below  $-32$  dB. It is difficult to assume that insects are constantly and evenly present throughout the entire layer up to 1600–2000 m throughout the day. This is statistically impossible.

This conclusion is confirmed by the results of computer simulation. The entire space up to 1600 m in height was divided into  $(1600/40)$   $12 = 480$  volume elements in accordance with the carried out radar measurements. It was assumed that this space contains  $N = 480n$  insects of the same size, on average  $n$  individuals in one volume element.

Let us consider the “idealized” case, which does not take into account the flocking behavior of insects and their non-uniform distribution near the ground, and assume that the distribution of insects over the volume elements is equally probable. What will be the statistics of their distribution across all elements?

Figure 5 shows the histograms of insect distributions by volume elements for the case  $N = 480 \times 3 = 1440$  and  $N = 480 \times 4 = 1920$ . It can be seen from the

diagrams that even with a uniform distribution of probabilities, some of the volume elements will be free of insects (tens of volume elements). Taking into account the schooling behavior of insects and their uneven distribution on the surface of Earth, in reality, the number of volume elements without insects should be even greater. Thus, if the radar signal were formed primarily by insects, then the radar reflectivity would fluctuate strongly and in insect-free volume elements would fall to  $Z = -55$  dBZ. This was not observed in our measurements; therefore, the background continual signal at a level from  $-32$  to  $-25$  dBZ was formed from fluctuations in the refractive index. Such levels of radar reflectivity are 15–20 dB higher than the maximum values given by Bragg’s theory for turbulent fluctuations.

In this paper, we only fix the facts and cannot explain the reasons for such a large discrepancy between experimental data and theory. To understand the physics of such results, apparently, it will be necessary to formulate and conduct complex studies.

## CONCLUSIONS

Thus, the experience of 20-year radar measurements of the wind field using a 35 GHz wind profiler is considered. The meteorological potential of the created radar has been substantiated, which makes it possible to record radar reflections from meteorological objects at an altitude of 1 km with radar reflectivity  $Z = -60$  dBZ. Particular attention is paid to reflections in a clear atmosphere. It is shown that in a number of cases the observed values of radar reflectivity from a clear sky cannot be explained by the existing turbulent theory of reflections from fluctuations of the refractive index. The discrepancies reach 15–20 dB. The current situation is quite predictable. The millimeter wavelength range lies at the limit of applicability of the theory of turbulence. In such cases, as a rule, other signal

generation mechanisms, which are not yet known, are brought to the fore. A probable explanation for the high level of radar reflectivity in field measurements may lie in the structure of thermals, which are formed due to uneven heating of the surface.

## REFERENCES

1. A. G. Gorelik and V. V. Kostarev, Dokl. AN SSSR **125**, 59 (1959).
2. D. Atlas, J. Atmos. Terr. Phys. **15** (3–4), 262 (1959).
3. D. Atlas, J. Meteorology **16** (1), 6 (1959).  
[https://doi.org/10.1175/1520-0469\(1959\)016<0006:ME>2.0.CO;2](https://doi.org/10.1175/1520-0469(1959)016<0006:ME>2.0.CO;2)
4. A. A. Chernikov, Trudy TsAO, No. 36, 126 (1961).
5. A. A. Chernikov, *Radar Reflections from the Clear Sky* (Gidrometeoizdat, Leningrad, 1979) [in Russian].
6. D. Atlas, *Advances in Radar Meteorology* (Gidrometeoizdat, Leningrad, 1967), ed. by H. E. Landsberg and J. Van Mieghem, in *Advances in Geophysics* (Academic, New York, 1964), Vol. 10, pp. 317–468.
7. V. D. Stepanenko, *Radar-Location in Meteorology* (Gidrometeoizdat, Leningrad, 1973) [in Russian].
8. A. G. Gorelik, L. V. Knyazev, and L. N. Uglova, Izv. AN SSSR, Ser. Fizika Atmosfery i Okeana. **9** (2) (1973).
9. P. Kollias, E. E. Clothiaux, M. A. Miller, et al., Bull. Am. Meteorolog. Soc. **88**, 1608 (2007).  
<https://doi.org/10.1175/BAMS-88-10-1608>
10. U. Górsdorf, V. Lehmann, M. Bauer-Pfundstein, et al., J. Atmospheric and Oceanic Technol. **32**, 675 (2015).
11. M. A. Kononov, *Small-Sized Doppler Radar Providing Wind Sensing of the Boundary Layer of the Atmosphere*, Cand. Sci. (Tech. Sci.) Dissertation (MGTU GA, Moscow, 2010).
12. V. V. Sterlyadkin and M. A. Kononov, Nauchn. Vestn. MGТУ GA, Ser. Radiofiz. i Radiotekh., No. 158, 5259 (2010).
13. V. V. Sterlyadkin, A. G. Gorelik, K. V. Kulikovskii, et al., in *Proc. Progress in Electromagnetics Research Symp.-Spring, St. Petetsburg, May 22–25, 2017* (IEEE, New York, 2017), p. 897.
14. V. V. Sterlyadkin, M. A. Kononov, and S. S. Bykovskii, Nauchn. Vestn. MGТУ GA, Ser. Radiotekhnika, No. 176, 31 (2012).
15. V. V. Sterlyadkin and K. V. Kulikovskii, in *Computer Science and Technology. Innovative Technologies in Industry and Informatics (Proc. Sci.-Tech. Conf., Moscow, Apr. 6–7, 2017)* (MTU-MIREA, Moscow, 2017), p. 633.
16. P. H. Hildebrand and R. S. Sekhon, J. Appl. Meteorol. & Climatol. **13**, 808 (1974).
17. V. I. Tatarskii, *Wave Propagation in Turbulent Atmosphere* (Nauka, Moscow, 1967) [in Russian].
18. *Radar in Meteorology*, Ed. by D. Atlas (Amer. Meteorol. Soc., Boston, 1990).
19. P. Kollias, Jo. Ieng, P. Borque, et al., J. Atmospher. & Oceanic Technol. **31**, 583 (2014).  
<https://doi.org/10.1175/JTECH-D-13-00045.1>
20. E. P. Luke, P. Kollias, K. L. Johnson, and E. E. Clothiaux, J. Atmospher. & Oceanic Technol. **25**, 1498 (2008).
21. V. V. Sterlyadkin, K. V. Kulikovskii, V. M. Kalmykov, and D. V. Ermilov, Ros. Tekhnol. Zh. **6** (6), 28 (2018).  
<https://doi.org/10.32362/2500-316X-2018-6-6-28-40>

*Translated by E. Seifina*